Molecular Biology of the Cell
Vol. 11, 2429–2443, July 2000

Luv1p/Rki1p/Tcs3p/Vps54p, a Yeast Protein That Localizes to the Late Golgi and Early Endosome, Is Required for Normal Vacuolar Morphology.

Michael J. Conboy and Martha S. Cyert*

Department of Biological Sciences, Stanford University, Stanford, California 94305-5020

Submitted February 29, 2000; Revised April 27, 2000; Accepted May 4, 2000
Monitoring Editor: Thomas D. Fox

We have characterized *LUV1/RKI1/TCS3/VPS54*, a novel yeast gene required to maintain normal vacuolar morphology. The *luv1* mutant was identified in a genetic screen for mutants requiring the phosphatase calcineurin for vegetative growth. *luv1* mutants lack a morphologically intact vacuole and instead accumulate small vesicles that are acidified and contain the vacuolar proteins alkaline phosphatase and carboxypeptidase Y and the vacuolar membrane H^+-ATPase. Endocytosis appears qualitatively normal in *luv1* mutants, but some portion (28%) of carboxypeptidase Y is secreted. *luv1* mutants are sensitive to several ions (Zn^{2+}, Mn^{2+}, and Cd^{2+}) and to pH extremes. These mutants are also sensitive to hygromycin B, caffeine, and FK506, a specific inhibitor of calcineurin. Some vacuolar protein-sorting mutants display similar drug and ion sensitivities, including sensitivity to FK506. Luv1p sediments at 100,000 × *g* and can be solubilized by salt or carbonate, indicating that it is a peripheral membrane protein. A Green Fluorescent Protein–Luv1 fusion protein colocalizes with the dye FM 4-64 at the endosome, and hemagglutinin-tagged Luv1p colocalizes with the *trans*-Golgi network/endosomal protease Kex2p. Computer analysis predicts a short coiled-coil domain in Luv1p. We propose that this protein maintains traffic through or the integrity of the early endosome and that this function is required for proper vacuolar morphology.

INTRODUCTION

The yeast vacuole or lysosome is an acidic, hydrolytic organelle that has many functions: osmoregulation, storage of nutrients, sequestration of toxins, and degradation and recycling of proteins, membrane, and carbohydrate. It is a dynamic and variable structure with several smaller clustered vacuoles found in growing cells; these coalesce into one large vacuole during cell stasis or low osmolarity (reviewed by Klionski *et al.*, 1990). Genetic screens for loss of vacuole structure or function have established that the vacuole is formed from several distinct paths of SNAP/SNARE-mediated transport. Screens for missorting of vacuolar proteases have identified peptidase-deficient mutants (*pep*) (Jones, 1977) and vacuolar protein-sorting mutants (*vps*) (Bankaitis *et al.*, 1986; Rothman and Stevens, 1986; Robinson *et al.*, 1988; Rothman *et al.*, 1989). Together, these genes define a clathrin-mediated pathway of vesicle transport from the Golgi, through the endosome or prevacuolar compartment (PVC), to the vacuole. An alternative, Adaptor Protein-3–mediated pathway is thought to bypass the endosome, leading from the late Golgi (*trans*-Golgi network [TGN]) directly to the vacuole (reviewed by Conibear and Stevens, 1998). Studies of endocytosis-defective mutants (*end*) have detailed the contribution to vacuole formation of actin-dependent endocytosis from the plasma membrane (reviewed by Wendland *et al.*, 1998). Two other modes of transport to the vacuole, cytoplasm-to-vacuole targeting and autophagocytosis, deliver cytoplasmic material either directly to the vacuole or through the endosome (reviewed by Klionski, 1998). Many of the same genes have been isolated in these different genetic screens, indicating that there is substantial overlap in these transport pathways. These studies, and others of vacuole morphology mutants (*vam*) (Wada *et al.*, 1992) or inheritance (*vac*) (Wiesman *et al.*, 1990; Gomes de Mesquita *et al.*, 1996), as well as in vitro assays of homotypic vacuole fusion (Nichols *et al.*, 1987), have helped define both the common biochemical mechanisms shared among the pathways and specific players for each trafficking step.

Mutations that disrupt traffic between the TGN and the vacuole, anterograde and retrograde, often result in vacuole fragmentation. Raymond and coworkers (1992) characterized the vacuole phenotypes of the various *vps* mutants and grouped them into six classes, expanding the three classes of Banta and coworkers (1988). Class D defines transport between the Golgi and the endosome/PVC; mutants in these genes have vacuoles that are thought to form from endocytic and

* Corresponding author. E-mail address: mcyert@leland.stanford.edu.

© 2000 by The American Society for Cell Biology

alkaline phosphatase (ALP) pathway traffic. Class E proteins mediate vesicle transport out of the PVC to the vacuole and retrograde back to the Golgi. Class E mutants thus accumulate PVC material, but transport to the vacuole is not completely blocked and vacuoles still form in these mutants (reviewed by Conibear and Stevens, 1998). Class B mutants show moderately fragmented vacuoles; many of the proteins defined by these mutations have been found as two complexes, called the retromer, which is thought to mediate retrograde transport from the PVC to the Golgi (Horazdovsky *et al.*, 1997; Seaman *et al.*, 1998). Class C mutants show severe vacuole fragmentation, and these proteins, Vps18p, Pep5p/Vps11p, Vps16p, and Vps33p, form the RING complex, which is thought to link vesicle targeting components together at the vacuole and may supply target specificity (Rieder and Emr, 1997). Class C mutants disrupt traffic from the PVC to the vacuole and thus also affect the late stages of endocytosis (Dulic and Reizman, 1990).

The membrane fusion events that occur during transport to the vacuole are mediated by SNARE proteins, together with additional regulatory and fusion factors (SNAPs, NSF, and RAB GTPases). For example, vesicle traffic from the Golgi to the PVC in yeast requires Pep12p (Becherer *et al.*, 1996) and Vti1p (Fisher von Mollard *et al.*, 1997) as the SNAREs, Vps21p as the RAB (Horazdovsky *et al.*, 1994; Singer-Kruger *et al.*, 1994), Vps45p as the Sec1p homologue (Cowles *et al.*, 1994; Piper *et al.*, 1994), and Sec17p and Sec18p as the ubiquitous SNAP and NSF. SNAREs and RABs are usually unique to a particular transport step, and the study of all the yeast SNAREs has shown in finer detail the vesicular sorting steps in yeast (reviewed by Pelham, 1999). For instance, Vam3p defines the vacuole, Pep12p defines the late endosome or PVC, Tlg1p and Tlg2p define the early endosome and/or the TGN, and Sed5p defines the early Golgi. However, it has also become apparent from such studies that neither SNAREs nor RABs alone supply the specificity in vesicle and target fusion (Grote and Novick, 1999). Rather, it is currently thought that the SNARE model requires additional, accessory proteins to recruit or tether the appropriate SNAREs and/or RABs, and thus the transport vesicle, to the appropriate target (reviewed by Waters and Pfeffer, 1999). The retromer and RING complexes mentioned above are currently thought to fill this role of targeting specificity.

Our laboratory studies the serine/threonine protein phosphatase type 2B, or calcineurin. Yeast strains lacking calcineurin are viable under standard growth conditions (Cyert *et al.*, 1991; Liu *et al.*, 1991; Cyert and Thorner, 1992). To identify genes that might compensate for the loss of calcineurin, a genetic screen was performed to identify mutations that are lethal in combination with a calcineurin mutation. Mutants defective in known genes were identified in this screen and subsequent analyses, including cell wall biosynthesis genes *fks1*, *kre5*, *kre6*, *kre9*, *mpk1*, and *vma* mutants (Garrett-Engele *et al.*, 1995; P. Garrett-Engele and M.S. Cyert, unpublished result). *VMA* genes encode subunits of the vacuolar membrane H^+-ATPase and are required for vacuole acidification. This acidification is required to activate vacuolar proteases and phosphatases and to drive ion sequestration. Calcineurin regulates cell wall biosynthesis and ion homeostasis at least in part through transcriptional activation of genes involved in these processes (Mendoza *et al.*, 1994; Cunningham and Fink, 1996; Matheos *et al.*, 1997; Stathopoulos and Cyert, 1997). Other mutants were also identified in the synthetic lethality screen described above; here we characterize the gene defined by one of those mutants, *LUV1/RKI1/TCS3/VPS54*, and present evidence that the protein it encodes mediates traffic through, or the stability of, the TGN or early endosome.

MATERIALS AND METHODS

Yeast Strains and Media

Yeast strains used in this study are listed in Table 1. Standard media and culture conditions were used (Sherman, 1991), except that twice the level of amino acids and nucleotides were added to synthetic media. Molecular cloning methods and yeast transformation were as described (Ausubel *et al.*, 1987). FK506 was from Fujisawa (Osaka, Japan). Sequencing reactions used Sequenase (United States Biochemical, Cleveland, OH) according to the manufacturer's protocol. PCR reactions used *Taq* polymerase from Life Technologies/BRL (Grand Island, NY) in a MJ thermal cycler (MJ Research, Watertown, MA). All restriction enzymes were from New England Biolabs (Beverly, MA).

Construction of luv1Δ Null

A *luv1Δ::hisGURA3hisG* allele was constructed in pBS-hisG-URA3-hisG (Alani *et al.*, 1987) by inserting a 1.8-kilobase (kb) *Sac*I–*Bgl*II fragment corresponding to a region just 5′ of the *LUV1* ORF into *Sac*I and *Bam*HI sites on one flank of the *hisGURA3hisG* cassette. On the other flank, a 1.5-kb *Pst*I–*Sal*I fragment corresponding to the C terminus and flank of *LUV1* was inserted into *Eco*RI and *Pst*I sites. The 7.2-kb *Sac*I–*Sal*I *luv1Δ::hisGURA3hisG* fragment was excised and transformed into diploid yeast MCY3, which is heterozygous for a calcineurin mutation. Diploids were sporulated, and the genotype of *luv1Δ::hisGURA3hisG* (strain YMC1) was confirmed by Southern analysis. To obtain strain YMC4, strain SF838-9DaR2L1 was transformed with the 7.2-kb *Sac*I–*Sal*I *luv1Δ::hisGURA3hisG* fragment and selected on uracil-free medium.

Construction of GFP-LUV1 Fusion

An N-terminal *GFP-LUV1* fusion was constructed with the use of PCR to amplify the *LUV1* coding region. N- and C-terminal specific primers contained *Bam*HI restriction sites, and the N-terminal primer was engineered to introduce a five-glycine linker before the first Luv1p methionine. The PCR product was digested with *Bam*HI and ligated to similarly digested pTS545 (Carminati and Stearns, 1997), which contains enhanced Green Fluorescent Protein (GFP) under the control of the *GAL1,10* promoter, to give plasmid pTS544::LUV1.

Construction of HA-LUV1

LUV1 contains a *Bgl*II restriction site at nucleotide 190. A 3X hemagglutinin (HA) fragment was amplified by PCR with the use of pTS515 (Marschall *et al.*, 1996) as a template and primers containing *Bgl*II restriction sites. The product was digested with *Bgl*II and ligated to similarly digested *LUV1* plasmid (in pRS315) (Sikorski and Hieter, 1989) to give pRS315*::LUV1::3XHA*.

Vacuole Staining and Immunofluorescence

For FM4-64 vacuolar staining, cells were grown in YPD to late log growth (OD_{600} = 5) to enhance vacuole structures. One OD_{600} unit of cells (i.e., the number of cells in 1 ml culture at OD_{600} = 1) was incubated on ice for 15 min with 32 μM FM4-64 dye (Molecular Probes, Eugene, OR) in 100 μl of YPD and washed in YPD at room temperature for 30 min as described (Vida and Emr, 1995). Similarly grown cells were incubated for 10 min with 2 μM quinacrine in pH 7.5 YPD as described (Roberts *et al.*, 1991). Cells were washed with

Table 1. Yeast strains used in this study

Strain	Relevant genotype	Source
YPH499	*MAT**a** ura3-52 lys2-801 ade2-101 trp*Δ*63 his3-*Δ*200 leu2*Δ*1*	Sikorski and Hieter (1989)
MCY3	*MAT**a**/*α *ura3-52/ura3-52 lys2-801/lys2-801 ade2-101/ade2-101 trp*Δ*63/trp*Δ*63/his3-*Δ*200/his3-*Δ*200 leu2*Δ*1/leu2*Δ*1 cnb1::LEU2*	Cyert and Thorner (1992)
PGY2	*MAT**a** ura3-52 lys2-801 ade2-101 trp*Δ*63 his3-*Δ*200 leu2*Δ*1 cna1*Δ*1::hisG cna2*Δ*1::HIS3 ade2* +pCNA2-29	Garret-Engele *et al.* (1995)
YMC1	*MAT**a** ura3-52 lys2-801 ade2-101 trp*Δ*63 his3-*Δ*200 leu2*Δ*1 luv1*Δ*::hisGURA3hisG*	This study
DBY4974	*MAT**a** ura3-52 lys2-801 his3-*Δ*200 leu2-3, 112*	D. Botstein
YMC2	*MAT**a** ura3-52 lys2-801 his3-*Δ*200 leu2-3, 112* + pTS545::*LUV1*	This study
YMC3	*MAT**a** ura3-52 lys2-801 ade2-101 trp*Δ*63 his3-*Δ*200 leu2*Δ*1* + pRS315::*LUV1::3XHA*	This study
SF838-9DaR2L1	*MAT**a** leu2-3, 112 ura3-52 his4-519 lys2 gal2 pep4-3*	T. Stevens
vps1	*MAT**a** leu2-3, 112 ura3-52 his4-519 lys2 gal2 pep4-3 vps1*Δ *(vps1)*	T. Stevens
pep5/vps11	*MAT**a** leu2-3,112 ura3-52 his4-519 lys2 gal2 pep4-3 vpl9-2 (pep5/vps11)*	T. Stevens
vps15	*MAT**a** leu2-3, 112 ura3-52 his4-519 lys2 gal2 pep4-3 vpl19-3 (vps15)*	T. Stevens
vps27	*MAT**a** leu2-3, 112 ura3-52 his4-519 lys2 gal2 pep4-3 vpl23-1 (vps27)*	T. Stevens
vps41	*MAT**a** leu2-3, 112 ura3-52 his4-519 lys2 gal2 pep4-3 vpl20-1 (vps41)*	T. Stevens
vps45	*MAT**a** leu2-3, 112 ura3-52 his4-519 lys2 gal2 pep4-3 vpl28-3 (vps45)*	T. Stevens
YMC4	*MAT**a** leu2-3, 112 ura3-52 his4-519 lys2 gal2 pep4-3 luv1*Δ*::hisGURA3hisG*	This study
YMC5	*vps27* (above) + *luv1*Δ*::hisGURA3hisG*	This study
YMC6	*MAT**a** leu2-3, 112 ura3-52 his4-519 lys2 gal2 pep4-3* + pTS545::*LUV1*	This study
YMC7	*vps27* (above) + pTS545::*LUV1*	This study
YMC8	YMC3 + pBMKX22	This study
YMC9	*vps27* (above) *luv1*Δ*::hisGURA3hisG*	This study
SEY6211a	*MAT**a** leu2-3, 112 ura3-52 his3*Δ*200 ade2-101 trp1*Δ*901*	S. Emr, via T. Stevens
vps17	*MAT**a** leu2-3, 112 ura3-52 his3*Δ*200 ade2-101 trp1*Δ*90 vpt3 (vps17)*	S. Emr, via T. Stevens
YMC10	*MAT**a** leu2-3, 112 ura3-52 his3*Δ*200 ade2-101 trp1*Δ*901 luv1*Δ*::hisGURA3hisG*	This study

pH 7.5 YPD and viewed under FITC fluorescence. For Vma, carboxypeptidase Y (CPY), and ALP immunofluorescence, similarly grown cells were fixed, permeabilized, and incubated as described (Piper *et al.*, 1997) with mouse mAbs to Vma2p, CPY, or ALP (Pho8p) (all from Molecular Probes). Secondary antibody was FITC donkey anti-mouse (Jackson Immunoresearch, West Grove, PA). GFP-Luv1p–expressing cells were grown in selective medium containing galactose and resuspended in YPD for one doubling before visualization or fixation. pBMKX22, a *URA* marked plasmid that contains *KEX2* under the *GAL* promoter, and anti-Kex2p antibody were generous gifts of R. Fuller (University of Michigan, Ann Arbor, MI) and were used as described (Redding *et al.*, 1991). Anti-Pep12 mAb was a generous gift from T. Stevens (University of Oregon, Eugene, OR) and was used at a 1:1000 dilution. Anti-HA antibody was acites fluid from Roche Molecular (Basel, Switzerland). FITC and Texas red–conjugated secondary antibodies were from Calbiochem (La Jolla, CA). Immunofluorescence, GFP, and FM4-64 were viewed on a Nikon (Garden City, NY) E600 microscope with the use of a Hammamatsu ORCA digital camera (Hamamatsu Photonics, Kyoto, Japan) and QED Imaging software (QED Imaging, Pittsburgh, PA) on an Apple (Cupertino, CA) Macintosh platform, and figures were prepared with the use of Adobe (Mountain View, CA) Photoshop.

CPY Sorting Assay

Metabolic labeling and immunoprecipitation of CPY immunoprecipitates were performed with the use of a method from the laboratory of T. Stevens (University of Oregon, Eugene, OR). One OD_{600} unit of early log-phase cells was incubated in 1 ml of Met-free and Cys-free synthetic medium, 50 mM potassium phosphate, pH 5.7, with 200 μCi of ^{35}S Trans-label (New England Nuclear, Boston, MA) and 2 mg/ml BSA. Cells were pulsed for 10 min at 30°C and chased by addition of 10 μg/ml cold Met and Cys for 40 min, whereupon labeling was terminated on ice with 10 μl of sodium azide. Cells were sedimented from the medium, and 100 μl of 10× IP buffer was added to the medium fraction (final concentration: 10 mM Tris, pH 8, 0.1% SDS, 0.1% Triton X-100, 2 mM EDTA, 0.5 mM PMSF, 1 μg/ml leupeptin, 1 μg/ml pepstatin). The cell fractions were converted to spheroplasts by incubating for 30 min at 30°C in 1.4 M sorbitol, 50 mM Tris, pH 7.4, 2 mM magnesium chloride, 10 mM sodium azide, 0.3% 2-mercaptoethanol, and 30 μg/ml Zymolyase 100T. Spheroplasts were lysed by boiling in 0.5% SDS and diluted to 1 ml in IP buffer (1× final concentration). Samples were boiled for 5 min and precleared with 20 μl of protein A–Sepharose, and CPY was immunoprecipitated by sequentially adding 0.5 μl of purified anti-CPY antiserum (a generous gift from the laboratory of R. Scheckman, University of California, Berkeley, CA) and 10 μl of protein A–Sepharose per sample with 1-h incubations for each. Immunoprecipitates were washed once through a 30% sucrose cushion in IP buffer and twice with plain IP buffer and resolved by SDS-PAGE; protein bands were imaged with the use of Kodak (Rochester, NY) X-AR film and quantified with the use of a Bio-Rad (Richmond, CA) CS screen and a Molecular Dynamics (Sunnyvale, CA) phosphoimager with Molecular Analyst software.

Protein Subcellular Fractionation

Cellular extracts were prepared essentially as described by Holthuis *et al.* (1998), who noted the addition of the energy poisons sodium fluoride and sodium azide to cells during spheroplasting. Early log-phase cells were sedimented, washed with 200 mM Tris, pH 8, 20 mM EDTA, 1% 2-mercaptoethanol, 5 mM sodium azide, and 5 mM sodium fluoride, converted to spheroplasts in the presence of 5 mM sodium azide and 5 mM sodium fluoride, and lysed by Dounce homogenization on ice in Tris/sorbitol buffer (50 mM Tris, pH 7.5, 200 mM sorbitol, 1 mM EDTA, with protease inhibitors added [1 μM each PMSF, pepstatin, benzamidine, 1 μg/ml each leupeptin, aprotinin, antipain, α-2-macroglobulin, and chymostatin]). Trypsin protease accessibility was determined by incubating cell extracts in

100 μl of 50 mM Tris, pH 7.5, 10 mM EDTA, 30 mM NaCl, 0.5% 2-mercaptoethanol, with or without L-1-tosylamide-2-phenylethyl-chloromethyl–treated trypsin, for 20 min at 25°C. Digestion was stopped by 10% trichloroacetic acid precipitation, and the proteins were identified by SDS-PAGE followed by Western blotting. For protein solubility, cell extracts were incubated on ice for 30 min in 150 μl of Tris/sorbitol buffer with the indicated compounds and then centrifuged for 30 min at 150,000 × *g*. For sucrose fractionation, 1 ml of extract from 50 ml of OD_{600} = 0.5 cells was layered onto 10 ml of a sucrose step gradient and buffered with 20 mM HEPES, pH 6.8, with steps of 1 ml at 60%, 2 ml each at 42, 36, 30, and 24%, and 1 ml at 18% sucrose (wt/wt). Gradients were centrifuged in an SW 41 rotor (Beckman Coulter, Fullerton, CA) at 150,000 × *g* for 18 h, and fractions were collected manually from the top. Sucrose concentration was determined on a Milton Roy (Ivyland, PA) refractometer (generously provided by R.T. Simoni, Stanford University, Stanford, CA). SDS-PAGE and Western blotting were performed with the use of Bio-Rad apparatus, Millipore (Bedford, MA) Immobilon membrane, antibodies at 1:1000 in TBS-Tween, 5% BSA, Amersham (Arlington Heights, IL) HRP-conjugated anti-mouse and anti-rabbit secondary antibodies (1:5000), and the Amersham ECL kit according to the directions of the manufacturer. Anti-HA mAb was from Roche Molecular and was used at a 1:1000 dilution. Anti-Kex2p was precleared against fixed *kex2*Δ yeast cells and used at a 1:500 dilution and detected robustly by sandwich amplification with the use of biotinylated anti-rabbit (1:1000) and HRP-streptavidin (1:1000) (Jackson Immunoresearch). Anti-Pep12p mAb was used at a dilution of 1:5000.

RESULTS

Cloning and Identification of LUV1/YDR027c

Previously, work from our laboratory identified mutants that depend on calcineurin for viability (Garrett-Engele *et al.*, 1995). These mutants were generated in strain PGY2, which contains null mutations in both calcineurin catalytic subunits (*cna1*Δ*1::hisG* and *cna2*Δ*1::HIS3*) but contains a plasmid-borne copy of *CNA2* that is galactose inducible. This study focuses on isolate #112 from that screen. Isolate #112 was transformed with a low-copy genomic *LEU2* library (American Type Culture Collection [Rockville, MD] 77162; F. Spencer and P. Hieter, unpublished), and colonies were selected for their ability to grow on dextrose, i.e., without calcineurin. Six complementing plasmid clones were obtained; sequencing of the end of each insert indicated that they overlapped an 11-kb region of chromosome IV (*Saccharomyces* Genome Database). Subcloning and testing for complementation narrowed the complementing DNA to a 4.5-kb *Sal*I–*Sac*I genomic fragment containing *YDR027c* (this gene has since been reported as *RKI1/TCS3/VPS54*; in this report, we refer to this gene as *LUV1*). We constructed a null mutation in this gene, *luv1*Δ, that deleted the ORF (see MATERIALS AND METHODS). A strain containing this null mutation failed to complement isolate #112 in a diploid, and tetrad analysis indicated that the mutations contained in these two strains were allelic and that the sporulation efficiency for the *luv1*Δ*/#112* diploid was unusually low. *luv1* mutants (both the original isolate and *luv1*Δ) were extremely slow growing (but viable) in strains lacking calcineurin. *luv1*Δ alleles were used in the following analysis, but isolate #112 showed similar phenotypes as *luv1*Δ strains for all aspects tested.

LUV1 Encodes a Novel Protein

LUV1 is predicted to encode an 889-amino acid protein (Figure 1A) with no predicted transmembrane domain, signal sequence, metal-binding site, or other identifiable motif (*Saccharomyces* Genome Database, Yeast Proteome Database, BLOCKS, MOTIF), except for a coiled-coil domain. Coils 2.1 (Lupas *et al.*, 1991) gave a strong prediction of a coiled coil in the region between amino acids 280 and 320 (Figure 1B), regardless of search window size, and weaker predictions of a coiled coil that vary depending on window size around amino acids 180, 340, and 680. XREF searches with the use of the Luv1 protein sequence revealed three homologues of similar size, *Schizosaccharomyces pombe* SPAC2F3.10 (EMBL), *Arabidopsis thaliana* ATF24J7.50 (EMBL), and *Caenorhabditis elegan*s CEY106G6H (EMBL), all proteins of unknown function. The strong prediction of a single coiled coil in the N-terminal third of the protein is shared with the homologues, which supports the prediction of this motif at this location in these proteins.

luv1 Shows Drug and Ion Sensitivities

Calcineurin mutants are sensitive to Na^+, $Li,^+$ Mn^{2+}, Cd^{2+}, and high pH and are resistant to calcium ion (Nakamura *et al.*, 1993; Breuder *et al.*, 1994; Cunningham and Fink, 1994; Mendoza *et al.*, 1994; Farcasanu *et al.*, 1995; Tanida *et al.*, 1995; Pozos *et al.*, 1996; Withee *et al.*, 1997, 1998). *vma* mutants, which like *luv1* were shown to require calcineurin function, share some of these calcineurin mutant phenotypes, including sensitivities to pH extremes, Zn^{2+}, Mn^{2+}, and Cd^{2+} (Anraku *et al.*, 1992; Garrett-Engele *et al.*, 1995). Therefore, we examined the growth properties of *luv1* mutants and found that they were sensitive to Zn^{2+}, Mn^{2+}, Cd^{2+}, and extremes in pH but not to Na^+ or Li^+ (Figure 2; our unpublished results). *luv1* was also sensitive to the drug FK506 (Figure 2), consistent with its requirement for calcineurin. Calcineurin mutants are sensitive to hygromycin B (Withee *et al.*, 1998), an aminoglycoside that inhibits protein translation. *luv1* mutants similarly showed sensitivity to hygromycin B (Figure 2). Additionally, *luv1* was sensitive to caffeine, a cAMP diesterase inhibitor, and failed to grow at high (37°C) and low (11°C) temperatures (Figure 2; our unpublished results). Calcium did not affect the growth of *luv1*; however, with an additional calcineurin mutation, the cells were very sensitive to this ion (our unpublished results). Unlike some of the genes shown to require calcineurin function, i.e., those involved in cell wall biosynthesis, *luv1* mutants were not sensitive to hypoosmotic stress (our unpublished results).

luv1 Mutants Show Vacuolar Morphology Defects

The ion sensitivities of *luv1* mutants are reminiscent of those of *vma* mutants and suggest that *luv1* mutants are defective for vacuole function. We visualized vacuolar structures in *luv1* cells with the use of the lipophilic dye FM4-64, which, at 25°C, is internalized in living cells through endocytosis, transported through the endosomal compartments, and accumulates at the vacuole (Vida and Emr, 1995). In wild-type cells at late log phase, numerous small vacuoles coalesce into one larger vacuole. When viewed under Nomarski differential interference contrast

A

```
MSISETPHNKSQGLQKAAGRPKIVVPEGSPSRNSDSGSFTIEGDTSLNDDL  50
LSISGSVTPRARRSSRLSLDSITPRRSFDSRTLSVANSRSFGFENETHSGS  100
MDFSPLGNNSIYEIVMNTRRKNWLNYPTVADIPQVSLSKNDLDDHWKTHVI  150
EYVKNIKSDYQIFQSTNNIRNMNQMEQLKELREGENMHEESFEANLRQGDA  200
ELINSIPDFYFSDKFQLDNPRTFHKVLDAIDLFLTKLDMKRQAERDEAFSE  250
LRDRLNDFLDIVETLLVTEISKSSHKFFHALSEVDNIQKRALDTMSELKEL  300
AQNIKTIDAENIRKKISHLEMIFKRKNVEKLEQGLLQAKLVLNKTDECKSM  350
YEENKLDNCLELIKSIDYLIKGDDSINEDVQSWTRCWPYKLSNLRTIPALS  400
ATREFLTNMKIEIGGKFSLQLSILLIDDLRSFCKSIKPKETLHRIQTGSND  450
KKQTIFTDNFSSKITELIVRLNRCEELTSAFDLYREKSITELKSIIKIYLP  500
TENAHADNNHDEKHLNNGSTSGSKLSRLIKEQTPAEFQSMLVNIFTHALEA  550
LRRLYGHQKLLLDISLNELASVKSPNENQHNMITQLDIRTGINEIIRIIQL  600
RTGKIIAVRRELNLSLRYDYFLKFYAICVIFIQECEVLSGEFLTKYLSNVL  650
ASQIKHYANAQSSKNYRNIKKKIDAEEWIPYIVDSSIQSDVNDIVSSIDID  700
PLSWTTILDMVGGSHDCENGRSEDKEKDEGNETYQGHRKSVVVGDKTFVAS  750
SSLLATIEVIKELNVLSINLPSIYLSNFEKLCYDALQYYNSSAMASVTQPG  800
NSLLKTGRNLSIMGESLDCLAEFVIIVQRFYQRLSNSNRDFEPFDASHYTT  850
LLGQFQASSNKIYMANAPPPPV  889
```

B

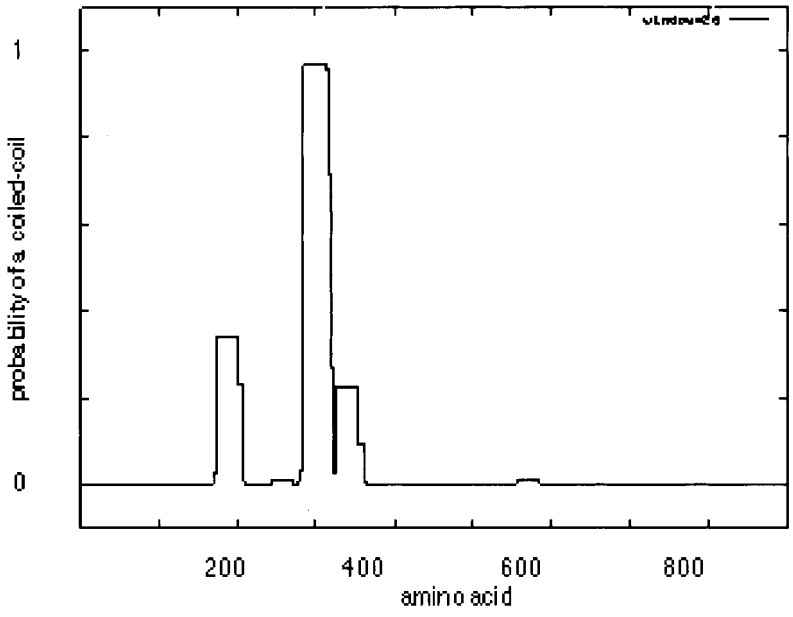

Figure 1. Computer predictions from *LUV1* sequence. (A) Predicted amino acid translation of *LUV1*. The putative coiled-coil region is underlined. (B) Coils 2.1 coiled-coil prediction for Luv1p.

microscopy, *luv1* cells did not have a visible vacuole. Instead, many (several tens) small vesicular bodies were seen dispersed throughout the cell; these vesicles also accumulated FM4-64 (Figure 3, FM4-64). Vesicles were also seen in daughter buds. Given the absence of a morphologically identifiable vacuole, we named this gene *LUV1* for Loss Upsets Vacuole.

We further examined *luv1* cells for vacuolar acidification and the presence of two vacuolar proteins, CPY and ALP. The vacuole lumen is acidified by the vacuolar H^+-ATPase, and the accumulation of a fluorescent dye, quinacrine, requires this acidification. *luv1* cells were incubated with quinacrine and viewed under fluorescence microscopy. Wild-type cells showed quinacrine fluorescence in large vacuolar structures, whereas *luv1* mutants displayed numerous punctate bodies of quinacrine staining (Figure 3, quinacrine). A similar, irregular punctate pattern was seen for the 60-kDa subunit of the membrane-bound vacuolar H^+-ATPase subunit, as detected by indirect immunofluorescence (Figure 3, Vma). CPY is a lumenal protease that is transported to the vacuole by a receptor, Pep1/Vps10p (Marcusson *et al.*, 1994; Horazdovsky *et al.*, 1995). In wild-type cells, CPY localized to the vacuole lumen; in *luv1* mutants, a punctate pattern was seen for CPY, as detected by indirect immunofluorescence (Figure 3, CPY). ALP is a membrane-bound protein that reaches the vacuole by an alternative pathway to CPY (Cowles *et al.*, 1997; Piper *et al.*, 1997;

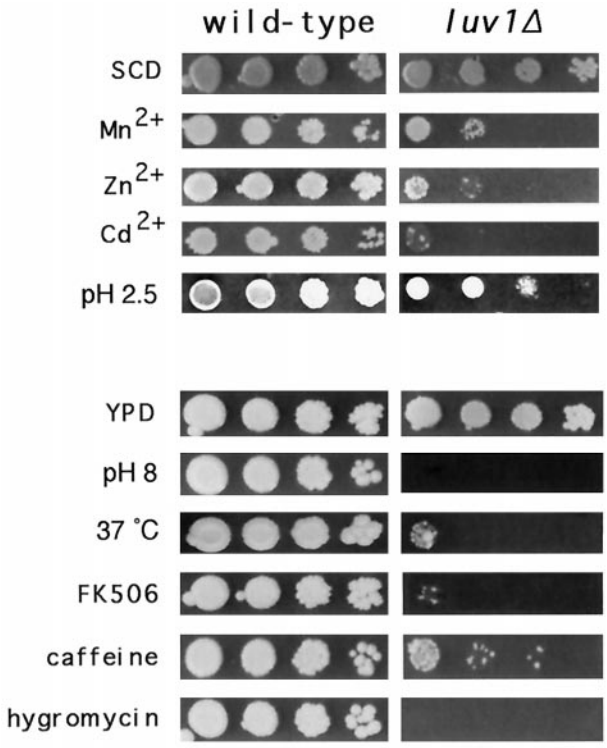

Figure 2. *luv1* mutant ion and drug sensitivities are characteristic of strains with vacuole defects. Serial 10-fold dilutions starting with OD_{600} = 1 of log-phase cells were spotted (5 μl) on solid medium with or without added ions or drugs as indicated. Plates were incubated at 25°C unless indicated otherwise and photographed at 10 d. Wild-type (YPH499) and *luv1*Δ (YMC1) strains are shown. Concentrations are as follows: Tris-HCl (pH 7.5), 50 mM; caffeine, 6 mM; FK506, 1 μg/ml; hygromycin B, 50 μg/ml (in yeast extract peptone medium); K_2HPO_4/KH_2PO_4 (pH 2.5), 50 mM; $MnCl_2$, 10 mM; $CdCl_2$, 0.2 mM; $ZnCl_2$, 4 mM (in synthetic complete dextrose medium).

Stepp *et al.*, 1997). Wild-type cells contained ALP at the vacuolar membrane, whereas in *luv1* mutants, punctate staining was observed (Figure 3, ALP). These observations all indicate that the vesicles observed in *luv1* mutants are fragmented vacuoles.

luv1 Missorts CPY

Class B and C *vps* mutants show moderate and severe vacuole fragmentation, respectively. In these mutants, 31 to 97% of total CPY is missorted (Raymond *et al.*, 1992), and as a consequence, it is secreted into the growth medium. Because *luv1* mutants showed vacuole fragmentation, we examined CPY processing and sorting in *luv1* cells. CPY is normally processed from a 67-kDa precursor (p1) in the endoplasmic reticulum to a fully glycosylated 69-kDa form (p2) in the Golgi. In the vacuole, precursors are cleaved to the 65-kDa mature (m) form by proteinase A (reviewed by Van Den Hazel *et al.*, 1996). The amount of CPY secreted by *luv1* was determined by metabolic labeling and immunoprecipitation. With the use of the method described (see MATERIALS AND METHODS), the *luv1* mutant (YMC10; Table 1) secreted 28% CPY into the medium (S) (Figure 4). This was substantially less than we observed for other *vps* mutants; for example, *vps17* (Table 1) secreted 89% CPY (our unpublished results). In *luv1* mutants, the correctly sorted CPY was mature, whereas missorted CPY was the fully glycosylated, Golgi-modified p2 form (Figure 4).

Some vps Mutants Require Calcineurin for Growth

luv1 mutants have fragmented vacuoles and missort CPY. In this way, *luv1* mutants resemble some *vps* mutants. We examined select *vps* mutants to determine if they exhibited drug and ion sensitivities similar to *luv1*. Representatives of each of the six phenotypic classes, A–F, were tested. *LUV1* was disrupted in the parental strain for comparison (to give YMC4). Many of the *vps* mutants also displayed growth properties similar to those of *luv1*, such as sensitivity to high temperature, pH extremes, hygromycin, Zn^{2+} (except *vps1*), and caffeine (except *vps1* and *vps45*) (Table 2). Unlike *luv1*, the *vps* mutants tested were not sensitive to Mn^{2+} or Cd^{2+}. Interestingly, some of the *vps* mutants were sensitive to FK506, indicating that they also require calcineurin function for viability. Although *vps35* (class A) and *vps17* and *vps41* (class B) showed the least severe vacuole defects and did not show FK506 sensitivity (our unpublished results), other *vps* mutants, such as *pep5/vps11* (class C), *vps15* and *vps45* (class D), and *vps1* (class F), did show FK506 sensitivity.

Luv1 Is Part of a High-Speed Pellet Fraction

To further characterize Luv1 protein function, we examined its localization in wild-type cells. We first characterized Luv1p subcellular localization through biochemical fractionation. An HA-tagged *LUV1* allele was constructed (see MATERIALS AND METHODS), and we determined that plasmid borne, low-copy *HA-LUV1* complements both the temperature-sensitive growth and fragmented vacuole phenotypes of *luv1* (our unpublished results). Western analysis of protein extracts from *HA-LUV1* cells showed a single predominant protein band at ~105 kDa. Most HA-Luv1 protein sedimented from cell extract at 100,000 × *g*, indicating that it may associate with a transport vesicle, Golgi, or early endosomal membrane fraction (Figure 5A). We attempted to solubilize HA-Luv1p by pretreating cell lysates with various chemicals before centrifugation at 150,000 × *g* into pellet (P) and supernatant (S) fractions. HA-Luv1p was partially solubilized after treatment with 2% Triton X-100 and was fully solubilized by 2% 3-([3-chloramidopropyl] dimethylammonio)-2-hydroxy-1-propanesulfonate, 1 M NaCl, and 0.1 M Na_2CO_3, pH 11 (Figure 5C). The salt and carbonate solubility suggests that Luv1p associates with the P100 fraction as a peripheral membrane protein. In support of this, the HA epitope was undetectable after trypsinization of cell extracts, indicating that at least the N terminus of Luv1p is accessible to protease (Figure 5B).

Luv1p Cofractionates with Kex2p

To further characterize the complex with which Luv1p associates, the 13,000 × *g* supernatant (S13) cellular fraction from HA-Luv1p–expressing cells was subjected to equilibrium sedimentation through a sucrose gradient. Fractions

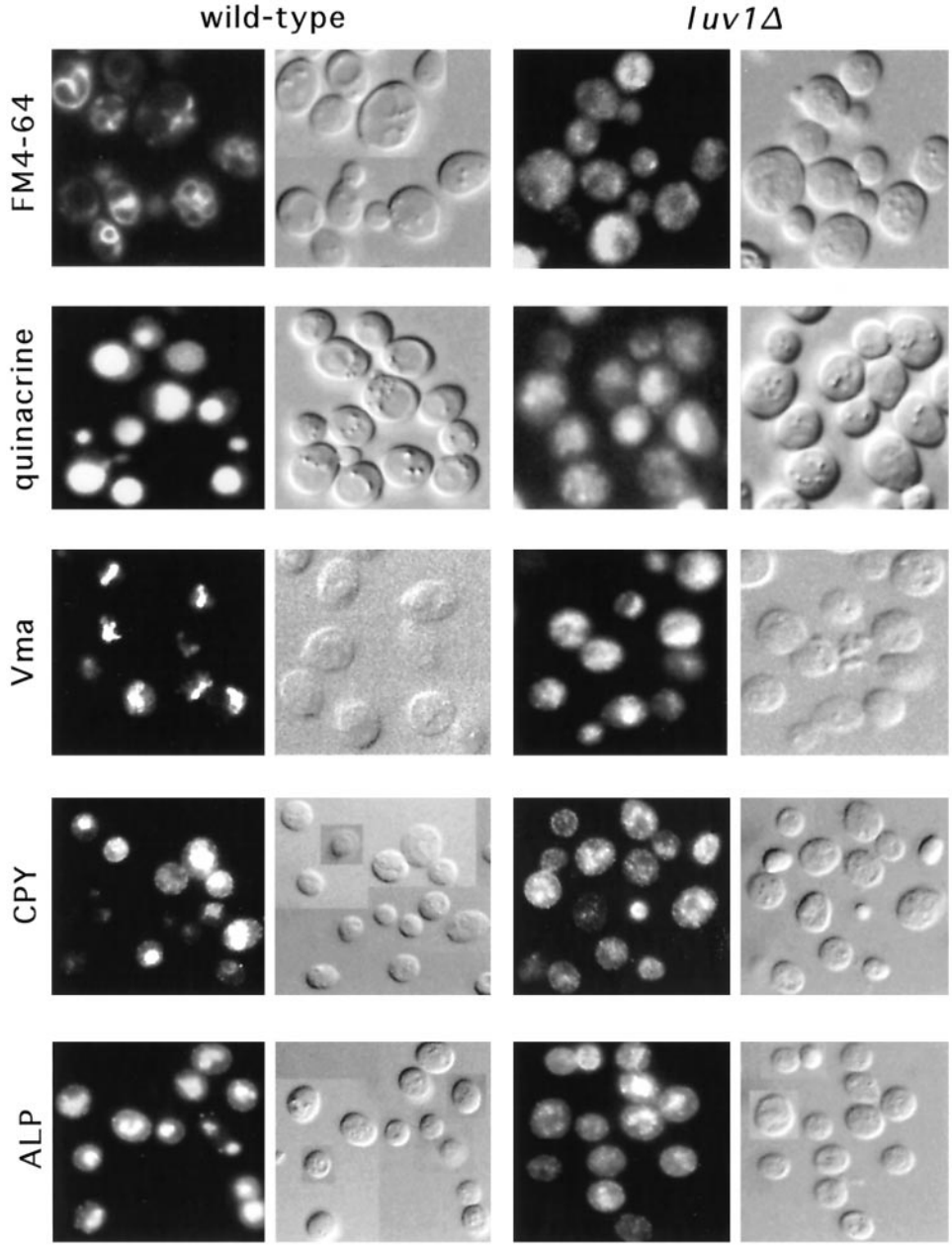

Figure 3. *luv1* mutants accumulate intracellular vesicles that are acidic and contain Vma2p, ALP, and CPY. Wild-type (YPH499) and *luv1*Δ (YMC1) cells were examined for vacuole morphology and characteristic vacuole proteins. Fluorescence and Nomarski differential interference contrast images are shown. FM4-64 indicates live cells labeled with this membrane dye to show vacuoles. Quinacrine indicates live cells loaded with this dye. Vma, CPY, and ALP indicate fixed cells in which the 60-kDa Vma2p subunit, CPY, and ALP, respectively, were localized by indirect immunofluorescence (see MATERIALS AND METHODS).

were collected and analyzed by SDS-PAGE and Western blotting. Anti-HA antibody detected HA-Luv1p in two peaks, the major peak between 20 and 25% sucrose and the minor peak at 35% sucrose (Figure 5D). Pep12p is a PVC t-SNARE that mediates vesicle traffic between the Golgi and the PVC (Becherer *et al.*, 1996). Anti-Pep12p antibody detected Pep12p in one peak that partially overlapped those fractions that contain the major peak of HA-Luv1p and did not detect Pep12p in the fractions that contain the minor peak of HA-Luv1p (Figure 5D). The protease Kex2p cycles between the TGN and an endosomal compartment (reviewed by Conibear and Stevens, 1998), and anti-Kex2p antibody detected Kex2p in the same fractions as HA-Luv1p, including the minor peak (Figure 5D). This indicates that Luv1p may be in the same subcellular structures as Kex2p (i.e., TGN and/or endosome) but is not in the same

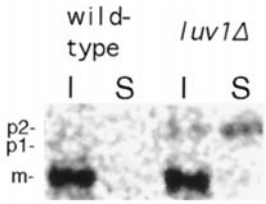

Figure 4. *luv1* mutants show a CPY protein-sorting defect. Wild-type (SEY6211a) and *luv1*Δ (YMC10) cells were pulsed or pulse-chased with [^{35}S]methionine/cysteine and converted to spheroplasts. Intracellular (I) and secreted (medium, S) fractions were prepared, immunoprecipitated with anti-CPY antibody, and resolved by SDS-PAGE and autoradiography (see MATERIALS AND METHODS). p1 indicates core glycosylated CPY; p2 indicates fully glycosylated CPY; m indicates mature CPY.

structures, or at least not all of the same structures, as Pep12p (i.e., PVC).

Luv1p Colocalizes with Kex2p

To determine the cellular localization of Luv1p, we fused GFP to Luv1p (see MATERIALS AND METHODS). Plasmid-borne, galactose-inducible *GFP-LUV1* complemented the growth defect of *luv1* mutants at 37°C and restored normal vacuolar morphology to this strain (our unpublished results). Cells expressing GFP-Luv1 protein showed the bulk of fluorescence as a few large dots visible inside the cell (Figure 6A, wt). Cells expressing GFP-Luv1p were fixed and immunostained to determine Pep12p localization. Pep12p was also detected as a few large dots inside the cell, although Pep12 dots did not colocalize with GFP-Luv1 dots (Figure 6A, wt, merge). In *vps27*, a class E *vps* mutant, prevacuolar material accumulates into a morphologically exaggerated PVC. In this mutant, Pep12p distribution is altered and accumulates in this exaggerated PVC (Piper *et al.*, 1995; Voos and Stevens, 1998) (Figure 6A). The GFP-Luv1p fluorescence pattern in the *vps27* mutant appeared the same as in wild-type cells (Figure 6A, *vps27*), indicating that Luv1p distribution is not altered in this mutant. Also, even in the *vps27* mutant, GFP-Luv1p did not colocalize with Pep12p (Figure 6A, *vps27*). Together, these results indicate that Luv1p does not localize with Pep12p at the PVC.

We next compared Luv1p and Kex2p subcellular localization by means of immunofluorescence. Cells expressing low-copy HA-Luv1p and overexpressing Kex2p were fixed and double immunostained for HA and Kex2p. Both anti-HA and anti-Kex2p immunofluorescence patterns appeared as a few dots inside the cell, and an overlay of separate HA and Kex2p images indicated a substantial overlap of HA-Luv1p and Kex2p localization (Figure 6B). This confirms that Luv1p and Kex2p colocalize in the yeast cell.

GFP-Luv1p Localizes to an Endosomal Compartment

As described above, the fluorescent lipophilic dye FM4-64 is endocytosed in living cells, travels through the endocytic pathway, and accumulates at the vacuole (Vida and Emr, 1995). Wild-type cells expressing GFP-Luv1p (YMC2) were loaded with FM4-64 dye and examined by fluorescence microscopy during the time course of FM4-64 endocytosis to the vacuole for GFP, FM4-64, or both. It was observed that GFP-Luv1p fluorescence colocalized with FM4-64 during that time course (our unpublished results). In cells held at 15°C, FM4-64 is endocytosed normally but accumulates at an endosomal compartment rather than at the vacuole (Vida and Emr, 1995). Wild-type cells expressing GFP-Luv1p were loaded with FM4-64 dye, incubated at 15°C, and again examined for GFP fluorescence, FM4-64, or both. At 15°C, most of the GFP dots also fluoresced with FM4-64, indicating colocalization (Figure 7, merge). This indicates that GFP-Luv1p localizes to the endosomal compartment that accumulates FM4-64 under these conditions and that the compartment containing Luv1p is part of the endocytic pathway.

vps27 luv1 Mutants Appear Morphologically Similar to luv1 Mutants

The *vps* class E mutations block transport out of the PVC both anterograde to the vacuole and retrograde to the Golgi; thus, these mutants accumulate an exaggerated PVC (reviewed by Conibear and Stevens, 1998). These mutants also have vacuoles that contain ALP, and the vacuoles are thought to form because the transport block to the vacuole is incomplete; in addition, the ALP pathway is still functional. We examined the effect of a *luv1* mutation on vacuolar morphology in a *vps27* (class E) mutant with the use of

Table 2. Drug and ion sensitivities

Strain	Class	37°C	pH 7.5	pH 2.5	Ca^{2+}	Mn^{2+}	Cd^{2+}	Zn^{2+}	Caffeine	FK506	Hygromycin
*luv1*Δ (strain YMC4)		−	−	−	+	−	−	−	−	−	−
vps1	F	+/−	−	−	+	+	+/−	+	+	−	−
pep5/vps11	C	−	−	−	−	+	+	−	−	−	−
vps15	D	−	−	−	+	+	+	−	−	−	−
vps27	E	+/−	+	−	+	+	+	−	−	+	−
vps45	D	−	−	−	+/−	+/−	+	−	+	−	−

Cell growth on plates with various added substances was assayed as in Figure 2. (+) Appreciable growth under these conditions compared with wild type; (−) no growth; (+/−) some growth. Classes are as described by Raymond *et al.* (1992). See Figure 2 for concentrations and conditions, calcium chloride 800 mM in synthetic complete dextrose medium.

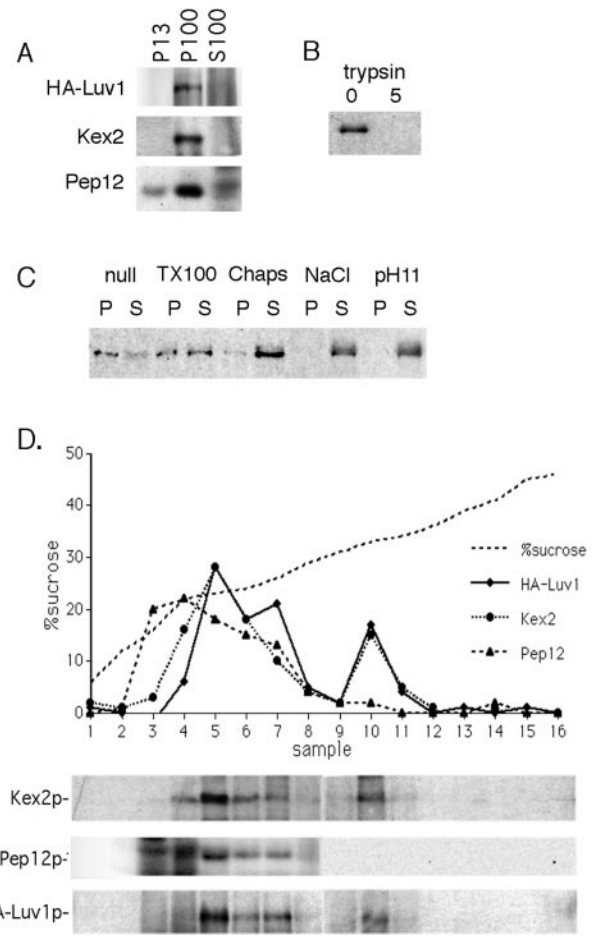

Figure 5. Biochemical analysis of Luv1p. (A) Luv1p sediments at 100,000 × *g*. Protein extract was prepared from cells containing CEN-based *HA-LUV1* (YMC3), and total lysates were sedimented sequentially to give a 13,000 × *g* pellet (P13), a 100,000 × *g* pellet (P100), and a supernatant (S100). Fractions were separated by SDS-PAGE and analyzed by Western blotting with the use of anti-HA, anti-Kex2p, and anti-Pep12p antibodies (see MATERIALS AND METHODS). (B) Luv1p is protease accessible. Total cell lysates from HA-Luv1p–expressing cells were treated with 0 and 5 μg of trypsin for 30 min at 25°C before analysis as in A. (C) Luv1p solubility. Total cell lysates from HA-Luv1p–expressing cells were incubated on ice for 30 min alone (null) or with 2% Triton X-100, 2% 3-([3-chloramidopropyl]dimethylammonio)-2-hydroxy-1-propanesulfonate (CHAPS), 1 M NaCl, or 0.1 M Na_2CO_3 (pH 11) before sedimentation at 150,000 × *g* to give pellet (P) and supernatant (S) fractions. Fractions were analyzed as in A. (D) Luv1p cofractionates with Kex2p. HA-Luv1p–expressing cells (YMC3) were lysed, and S13 fractions were prepared and subjected to equilibrium sedimentation through a sucrose gradient. Fractions were analyzed by SDS-PAGE, followed by Western blotting with anti-HA, anti-Kex2p, and anti-Pep12p antibodies. The intensities of protein bands are shown in the graph, and the sucrose concentrations of the recovered fractions are also indicated.

FM4-64 dye. Cells were loaded with dye at 25°C to promote full endocytosis of the dye and accumulation at vacuolar structures. Wild type (SF838-9DaR2L1) and *vps27* mutants showed FM4-64 staining of large, lobed, normal vacuolar structures, whereas *luv1* mutants (YMC4) showed vacuolar fragmentation (Figure 8). In contrast to *vps27* or the parental strain, the *vps27 luv1* double mutant (YMC9) showed FM4-64 staining very similar to that of the *luv1* single mutant, with numerous small vesicles and no visible vacuolar structures (Figure 8). Also, as seen in *luv1* mutants (Figure 3), the vesicles seen in the *vps27 luv1* double mutant stained with quinacrine, indicating that they are acidified (our unpublished results). This suggests that the same vacuolar fragmentation seen in the *luv1* single mutant also occurs in the *vps27 luv1* double mutant.

DISCUSSION

We have isolated a mutant of *LUV1/RKI1/TCS3/VPS54/YDR027c* that requires calcineurin for viability. To identify the function of the *LUV1* gene product, we characterized the *luv1* mutant, localized the Luv1 protein, and characterized biochemical properties of the protein. We propose that Luv1p acts at the late Golgi and early endosome to mediate the integrity of, or transport through, these compartments.

Loss of Luv1p Leads to Vacuole Defects and Fragmentation

luv1 mutants display ion phenotypes (Figure 2) that suggest some loss of vacuole function in these cells. The Mn^{2+}, Zn^{2+}, and Cd^{2+} sensitivities of *luv1* mutants suggest that these ions are not effectively sequestered to the vacuole. These sensitivities may result from a loss of polyphosphate, which is thought to help sequester ions in the mature vacuole (reviewed by Klionski *et al.*, 1990), or from a loss of vacuolar integrity. Many of these sensitivities are shared with *vps* mutants (Table 2), especially those that, like *luv1*, show severely disrupted vacuolar morphology. We show here that *luv1*, calcineurin, and some *vps* mutants are sensitive to the aminoglycoside hygromycin B. This sensitivity is likely not due to the effect of this drug on protein translation, because *luv1* and calcineurin mutants show no sensitivity to cycloheximide, which inhibits translation. Dean (1995) has reported that glycosylation-defective mutants are sensitive to aminoglycoside drugs. However, *luv1* shows correct CPY and ALP processing, indicating that the hygromycin sensitivity is not a result of glycosylation defects. In mammalian cells, aminoglycoside drugs, including hygromycin, have been shown to interfere with coatomer (COPI) coat formation and secretion (Hudson and Draper, 1997; Hu *et al.*, 1999). Yeast COPI mediates retrograde vesicle transport from the Golgi to the endoplasmic reticulum (reviewed by Cosson and Letourneur, 1997). Perhaps hygromycin B inhibits the growth of some *vps*, *luv1*, and glycosylation-defective mutants by interfering with COPI-mediated transport.

luv1 mutations cause severe vacuolar fragmentation, yet the fragments seen in the *luv1* mutant contain characteristic vacuolar proteins: the vacuolar H^+-ATPase, CPY, and ALP (Figure 3). The presence of the vacuolar H^+-ATPase and vesicle acidification in *luv1* cells indicates that the vacuolar H^+-ATPase assembles and functions in *luv1* mutants. Others have recently characterized *luv1/tcs3/vps54* mutants and also noted vacuole defects (Bensen *et al.*, 2000; Conibear and Stevens, 2000). Bensen *et al.* (2000) isolated *luv1/tcs3* in a screen for synthetic lethality with a temperature-sensitive,

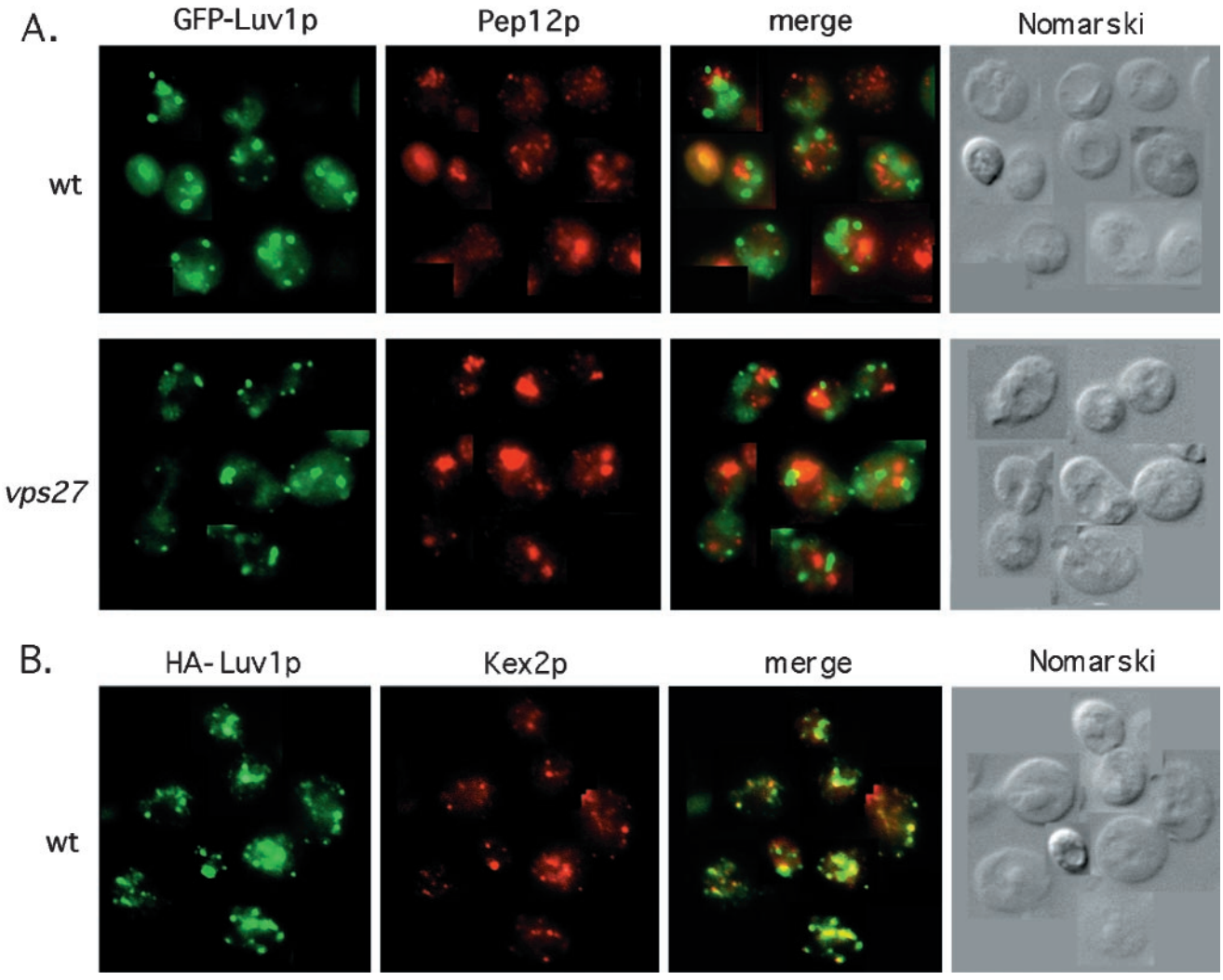

Figure 6. Intracellular localization of Luv1p. (A) GFP-Luv1p does not colocalize with Pep12p in wild type or *vps27* mutants. Fixed wild-type (YMC6) or *vps27* (YMC7) cells expressing GFP-Luv1p were immunostained for Pep12p and visualized for GFP (green) or Pep12p (red) in separate channels. Overlays of the separate images (merge) and Nomarski differential interference contrast images are also shown. (B) HA-Luv1p and Kex2p colocalize. Wild-type cells expressing HA-Luv1p and overexpressing Kex2p (YMC8) were immunostained for HA (green) and Kex2p (red) and visualized as in A.

partial-loss-of-function clathrin mutation. They found that *luv1/tcs3* mutants show a defect in CPY sorting, in agreement with our findings, and also that ALP processing and sorting is normal in *luv1/tcs3* mutants. Similarly, Conibear and Stevens (2000) reported no gross defects in ALP processing and sorting in *luv1/vps54* and no defects in invertase secretion, although they noted significantly more CPY secretion. Either strain or protocol differences may account for these quantitative differences; however, qualitatively, both of these studies are consistent in finding that *luv1* mutants show a CPY protein-sorting defect. Because the *luv1* mutation appears to affect CPY sorting more than ALP and does not affect secretion at all, Luv1p may be required at a step after the CPY pathway diverges from the secretory and ALP pathways.

Luv1 Protein

The *LUV1* gene product is predicted to contain a coiled-coil domain. Coiled coils are features shared by SNAREs and intermediate filament proteins. However, Luv1p does not otherwise resemble a SNARE, because it is much larger than SNARE proteins, lacks a transmembrane domain, and is solubilized by salt or high pH (Figure 5C). Luv1p does not resemble cytoskeletal proteins either, because the coiled-coil region is relatively small and is not predicted to form a structural rod. Nevertheless, there are several proteins that, like Luv1p, lack identifying functional motifs except for an N-terminal coiled coil (Figure 1B). Members of the exocyst complex, some *vps* class C proteins, and many *vps* class E proteins share this feature. The exocyst complex is a multimer of at least seven proteins (Bowser and Novick, 1991;

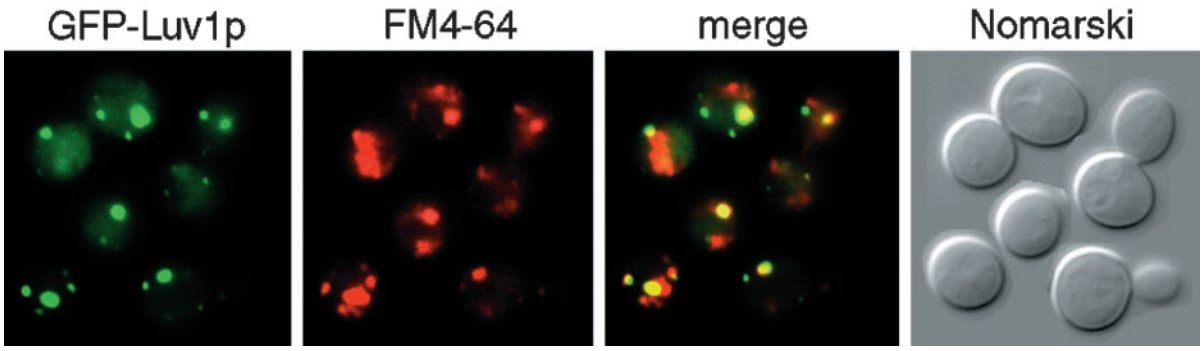

Figure 7. Luv1p localizes to an endosomal compartment. Live wild-type cells (YMC6) expressing a GFP-Luv1 fusion protein were incubated with the dye FM4-64 at 14°C to promote dye accumulation at the prevacuole. GFP, FM4-64 fluorescence, an overlay of the separate images (merge), and a Nomarski differential interference contrast image are indicated.

Bowser *et al.*, 1992; TerBush and Novick, 1995) that is thought to target transport vesicles to a specific intracellular location, the bud tip, by mediating vesicle–cytoskeleton interactions (TerBush *et al.*, 1996). Although an exocyst-like complex has not been found at the PVC or vacuole, it has been proposed that the *vps* class C RING complex functions similarly to target vesicle fusion to a specific subregion of the vacuole (Rieder and Emr, 1997). Several of the components of the RING complex, Pep5/Vps11p, Vps16p, and Pep3/Vps18p, have predicted short coiled-coil motifs (Rieder and Emr, 1997). Perhaps Luv1p is part of an analogous complex at the TGN/early endosome (see below). The biochemical characteristics of Luv1p are consistent with this suggestion. Luv1p sediments with a high-speed pellet fraction (Figure 5A, P100), suggesting that it associates with transport vesicles, Golgi, and/or early endosome. Luv1p is solubilized from this fraction by treatment with high pH or salt (Figure 5C), indicating that it is a peripheral membrane protein. Recently, others have identified two proteins with which Luv1/Vps54p associates: Sac2/Vps52p and Vps53p (Conibear and Stevens, 2000). We also detected two proteins of the approximate molecular weight of Sac2/Vps52p and Vps53p in immunoprecipitations of HA-Luv1p (our unpublished results).

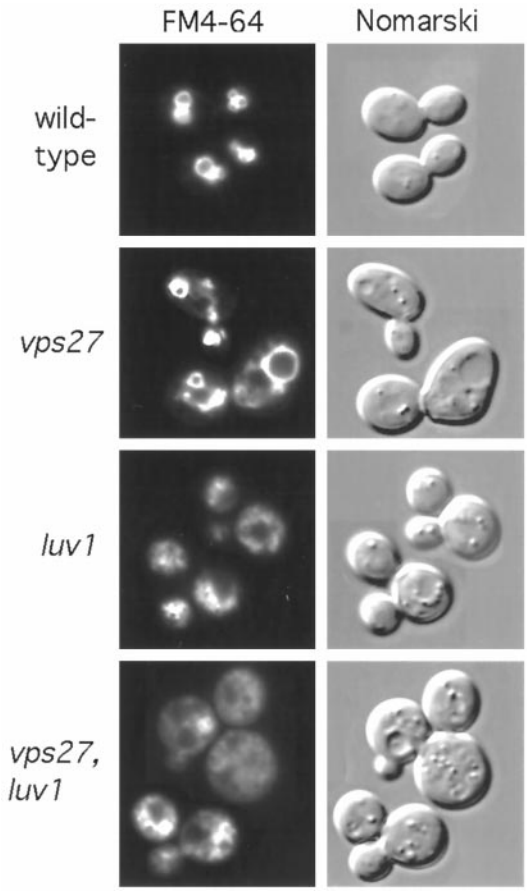

Figure 8. *vps27 luv1*Δ double mutants appear morphologically similar to a *luv1*Δ single mutant. Live wild-type (SF838-9DaR2L1), *vps27*, *luv1*Δ (YMC4), and *vps27 luv1*Δ (YMC9) cells labeled with FM4-64 dye at 25°C are shown under fluorescence (FM4-64) and Nomarski differential interference contrast microscopy.

Like *luv1*, some of the class B *vps* mutants show vacuole fragmentation into numerous vesicles that are acidified and contain ALP (Raymond *et al.*, 1992), and by these criteria, *luv1* could be classified as a *vps* class B mutation. A complex of several class B Vps proteins, called the retromer, has been characterized to be required for endosome-to-Golgi recycling of membrane and cargo (Seaman *et al.*, 1998; reviewed by Conibear and Stevens, 1998). Although Luv1p has not been found as part of the retromer complex, its localization and mutant phenotypes suggest that it may be involved at the same organelle or sorting step.

Model for Luv1p Function

Most of the Luv1 protein shows colocalization with the TGN protease Kex2p (Figure 6B) and cofractionates on a sucrose gradient with Kex2p (Figure 5D). In agreement with this, Conibear and Stevens (2000) also report that Luv1/Vps54p colocalizes with the marker protein A-ALP at the TGN. Luv1p also appears to localize to an endosomal compartment, as demonstrated by substantial colocalization of a GFP-Luv1 fusion protein with FM4-64 dye in wild-type cells kept at 15°C (Figure 7). However, this

endosomal compartment is not the late endosome or PVC, because no colocalization was seen of GFP-Luv1p and the PVC t-SNARE Pep12p, even in a *vps27* mutant (Figure 6A) that accumulates Pep12p in an exaggerated PVC (Piper *et al.*, 1995; Voos and Stevens, 1998). Thus, we conclude that Luv1p localizes to both the TGN and an endosomal compartment. Others have shown that the endosomal/TGN syntaxin Tlg2p and FM4-64 colocalize very well at 15°C (Abeliovich *et al.*, 1998) and that Tlg2p and Kex2p colocalize well (Holthuis *et al.*, 1998; Lewis *et al.*, 2000). The Golgi marker Sec7p was also shown to colocalize with FM4-64 dye at early stages of endocytosis, and Sec7p showed some colocalization with Tlg2p (Lewis *et al.*, 2000). None of these proteins were shown to localize to the late endosome/PVC. These findings suggest that Luv1p, Kex2p, Tlg2p, Sec7p, and FM4-64 at 15°C may all colocalize in the cell at an early endosomal compartment and/or the TGN.

One current model of intracellular transport in yeast takes into account the existence of such an early endosome that is distinct from both the late endosome/PVC and the late Golgi/TGN (reviewed by Pelham, 1999). In this model, the TGN is where the secretory pathway and both the CPY and ALP vacuolar targeted pathways diverge, whereas the early endosome is where the CPY branch of vacuolar traffic meets endocytic traffic and where retrograde traffic flows back to the TGN. In this model, the Golgi does not directly receive endocytic traffic, and the late endosome/PVC does not directly receive TGN traffic, because both endocytic and TGN traffic are presorted through the early endosome. Within the framework of this model, we propose that Luv1 protein is required to stabilize and/or localize the early endosomal compartment and that *luv1* phenotypes can be explained by mislocalized or abnormal early endosome, which subsequently matures to have vacuolar characteristics. Our reasoning is as follows. First, as described above, the *luv1* mutation appears to preferentially affect the pathway defined by CPY transport, as opposed to the secretory or ALP pathway. This would suggest that Luv1p functions after the secretory and ALP transport pathways diverge from the CPY pathway, or after the TGN. Second, the vesicles visible in *luv1* mutants display properties characteristic of vacuoles, yet they also rapidly accumulate FM4-64 dye at 15°C as at higher temperatures (our unpublished results, but compare with Figure 3). Thus, these vesicles also appear to have properties of early endosomes. Third, two additional defects have been noted in *luv1/tcs3* mutants (E. Bensen and G. Payne, personal communication). One defect is a kinetic delay in Ste3p turnover. This indicates that there is an endocytosis defect in *luv1/tcs3* mutants that compromises transport at some point between the plasma membrane and the vacuole. The other defect is that *luv1/tcs3* mutants have reduced α-factor processing due to reduced stability of the Golgi-localized protease Kex2p (Bensen *et al.*, 2000). This finding suggests that *luv1/tcs3* cells have defects either in some step of retrograde transport between the early endosome and the Golgi or in sorting from the Golgi to the early endosome (reviewed by Wilsbach and Payne, 1993). Similarly, Conibear and Stevens (2000) noted proteolysis of Pep1p/Vps10p and the model protein A-ALP in *luv1* mutants, indicating that retrieval from an endocytic compartment to the Golgi was impaired. Together, these defects suggest that in the absence of Luv1p, transport out of the early endosome is disrupted, in both directions, to the vacuole and back to the TGN. Fourth, the class E *vps27* mutation incompletely blocks anterograde transport out of the PVC to the vacuole; thus, *vps27* mutants still form vacuoles (reviewed by Conibear and Stevens, 1998). We find that a *vps27 luv1* double mutant appears morphologically like a *luv1* mutant, with an accumulation of many small vacuole-like vesicles but no large vacuole (Figure 8). This observation suggests that *luv1* disrupts an earlier compartment than the class E PVC or disrupts the remaining vacuolar transport in the *vps27* mutant. Finally, we note that *luv1* suffers growth defects at 37°C, at which temperature wild-type cells will accumulate endosomes (Mulholland *et al.*, 1999). Together, these observations suggest that Luv1p acts to localize, stabilize, or facilitate traffic through the early endosome in wild-type cells, in *vps27* mutants, and perhaps at high temperatures.

An alternative model that has been used to explain intracellular transport to the vacuole describes a single transport step from the TGN to the late endosome/PVC, another step from the plasma membrane to the late endosome/PVC (endocytosis), and retrograde transport from the late endosome back to the TGN (reviewed by Conibear and Stevens, 1998). This model does not specify the involvement of an early endosome in transport to the vacuole. Within the framework of this model, Conibear and Stevens (2000) have proposed that Luv1p/Vps54p acts to facilitate retrograde transport from the late endosome/PVC to the TGN. We have expanded this view of Luv1p function to incorporate the finding that the Luv1p-containing compartment also receives early endocytic traffic.

Luv1p and Microtubules

A recent report suggests that Luv1p may interact with microtubules. Smith and coworkers (1998) isolated *luv1/rki1* in a synthetic lethal screen with an *rbl2* null mutant. They reported that *luv1/rki1* null mutants show phenotypes consistent with microtubule defects, namely spindle defects, incomplete tetrad formation from homozygous *rki1*Δ diploids, and sensitivity to cold (15°C) and the microtubule-depolymerizing drug benomyl. In our strain background, *luv1* did not show benomyl sensitivity (our unpublished results). Smith *et al.* also demonstrated that Rbl2p binds in vitro to Luv1p/Rki1p and β-tubulin. However, neither Conibear and Stevens (2000) nor ourselves (our unpublished results) detected Rbl2p or β-tubulin in immunoprecipitates of Luv1/Vps54p. The role of microtubules in vesicle transport, organelle movement, and maintenance is well established in mammalian cell systems (reviewed by Bloom and Goldstein, 1998). In yeast, however, there are few studies implicating microtubules in vesicle transport: microtubules may be involved in autophagosome travel to the vacuole (Lang *et al.*, 1998), and Golgi fragmentation has been reported in cells with disrupted microtubules (Rambourg *et al.*, 1996). Any involvement with Luv1p/Rki1p with microtubules in transport is unclear and awaits further investigation.

LUV1 and Calcineurin Synthetic Lethality

We and others find that *luv1*, *vma*, and several *vps* mutants are FK506 sensitive and thus require calcineurin for viability

(Table 2) (Garrett-Engele *et al.*, 1995; Hemenway *et al.*, 1995). Why do mutants that disrupt vacuolar function require calcineurin? One major function of calcineurin is activation of the Crz1p transcription factor, which results in increased expression of several genes, including *PMC1*, a vacuolar Ca^{2+}-ATPase (Matheos *et al.*, 1997; Stathopoulos and Cyert, 1997). The growth of *vma2 crz1* double mutants is severely compromised (A.M. Stathopoulos and M.S. Cyert, unpublished results), and the FK506 sensitivity of *vma2* mutants is suppressed by overexpression of *PMC1* (L. Chen and M.S. Cyert, unpublished results). Thus, *vma* mutants seem to require calcineurin solely for its ability to promote *PMC1* expression. In contrast, we found that the growth of a *luv1 crz1* double mutant was equivalent to that of a *luv1* mutant (16 tetrads dissected) and that the FK506 sensitivity of *luv1* mutants was not suppressed by overexpression of either *PMC1* or *PMR1* (our unpublished results), the latter a Golgi-localized Ca^{2+}-ATPase whose expression is also regulated by calcineurin via Crz1p (Matheos *et al.*, 1997; Stathopoulos and Cyert, 1997). These observations suggest that calcineurin/Crz1p-regulated gene expression is not required for the viability of *luv1* mutants. Thus, the role of calcineurin in maintaining *luv1* mutant viability remains to be elucidated. Calcineurin has been shown to regulate vesicle transport in higher eukaryotic systems and to dephosphorylate several proteins required for clathrin-mediated vesicle recycling: dynamin, amphiphysin, and synaptojanin (reviewed by Marks and McMahon, 1998). The GTPase dynamin is generally thought to pinch or sever the neck of the developing vesicle, synaptojanin is a phosphatidylinositol phosphatase thought to modify lipid phosphate to recruit components to a site of vesicle budding, and amphiphysin is thought to recruit dynamin. Yeast cells do contain homologues of these proteins, and the dynamin Vps1p and the synaptojanin Inp53p are thought to act in trafficking from the Golgi to the vacuole (Conibear and Stevens, 1998; Bensen *et al.*, 2000). However, in yeast, no studies have yet defined a role for calcineurin in the regulation of these proteins. In light of the work by Bensen and coworkers (2000), showing that a *luv1/tcs3* mutation is synthetically lethal with a clathrin mutation, and our results, a possible role of yeast calcineurin in a clathrin-mediated vesicle transport process is particularly intriguing.

ACKNOWLEDGMENTS

We express our gratitude to T. Stearns for generously providing reagents, equipment, and advice, to E. Bensen, G. Payne, E. Conibear, and T. Stevens for selflessly sharing results and interpretations before publication, and to K. Bartz, T. Stevens, T. Sato, T. Darsow, S. Emr, K. Blumer, K. Redding, R. Fuller, E. Jones, and M. Rexach for reagents or reagent-grade discussion. We acknowledge the *Saccharomyces* Genome Database (Cherry *et al.*, 1998) and the Yeast Protein Database (Costanzo *et al.*, 2000) as being invaluable information resources for this work. M.J.C. was supported by National Institutes of Health grant 5 T32 GM07276. M.S.C. was supported by biomedical scholar award 92-42 from the Lucille P. Markey Charitable Trust, National Science Foundation Young Investigator award MCB-9357071, and funds from the Proctor and Gamble Company. This work was funded by National Institutes of Health research grant GM-48729 (to M.S.C.), which was also a source of support for M.J.C.

REFERENCES

Abeliovich, H., Grote, E., Novick, P., and Ferro-Novick, S. (1998). Tlg2p, a yeast syntaxin homolog that resides on the Golgi and endocytic structures. J. Biol. Chem. *273*, 11719–11727.

Alani, E., Cao, L., and Kleckner, N. (1987). A method for gene disruption that allows repeated use of *URA3* selection in the construction of multiply disrupted yeast strains. Genetics *116*, 541–545.

Anraku, Y., Hirata, R., Wada, Y., and Ohya, Y. (1992). Molecular genetics of the yeast vacuolar H^+-ATPase. J. Exp. Biol. *172*, 67–81.

Ausubel, F.M., Brent, R., Kingston, R.E., Moore, D.D., Seidman, J.G., Smith, J.A., and Struhl, K. (eds.) (1987). Current Protocols in Molecular Biology, New York: John Wiley & Sons.

Bankaitis, V.A., Johnson, L.M., and Emr, S.D. (1986) Isolation of yeast mutants defective in protein targeting to the vacuole. Proc. Natl. Acad. Sci. USA *83*, 9075–9079.

Banta, L.M., Robinson, J.S., Klionsky, D.J., and Emr, S.D. (1988). Organelle assembly in yeast: characterization of yeast mutants defective in vacuolar biogenesis and protein sorting. J. Cell Biol. *107*, 1369–1383.

Becherer, K.A., Rieder, S.E., Emr, S.D., and Jones, E.W. (1996). Novel syntaxin homologue, Pep12p, required for the sorting of lumenal hydrolases to the lysosome-like vacuole in yeast. Mol. Biol. Cell *7*, 579–594.

Bensen, E.S., Costaguta, G., and Payne, G.S. (2000). Synthetic genetic interactions with temperature-sensitive clathrin in *Saccharomyces cerevisiae*: roles for synaptojanin-like Inp53p and dynamin-related Vps1p in clathrin-dependent protein sorting at the *trans*-Golgi network. Genetics *154*, 83–97.

Bloom, G.S., and Goldstein, L.S.B. (1998). Cruising along microtubule highways: how membranes move through the secretory pathway. J. Cell Biol. *140*, 1277–1280.

Bowser, R., Müller, H., Govindan, B., and Novick, P. (1992). Sec8p and Sec15p are components of a plasma membrane-associated 19.5S particle that may function downstream of Sec4p to control exocytosis. J. Cell Biol. *118*, 1041–1056.

Bowser, R., and Novick, P. (1991). Sec15 protein, an essential component of the exocyst apparatus, is associated with the plasma membrane and with a soluble 19.5S particle. J. Cell Biol. *112*, 1117–1131.

Breuder, T., Hemenway, C.S., Movva, N.R., Cardenas, M.E., and Heitman, J. (1994). Calcineurin is essential in cyclosporin A- and FK506-sensitive yeast strains. Proc. Natl. Acad. Sci. USA *91*, 5372–5376.

Carminati, J.L., and Stearns, T. (1997). Microtubules orient the mitotic spindle in yeast through dynein-dependent interactions with the cell cortex. J. Biol. Chem. *138*, 629–641.

Cherry, J.M., *et al.* (1998). *SGD: Saccharomyces* Genome Database. Nucleic Acids Res. *26*, 73–79.

Conibear, E., and Stevens, T.H. (1998). Multiple sorting pathways between the late Golgi and the vacuole in yeast. Biochim. Biophys. Acta *1404*, 211–230.

Conibear, E., and Stevens, T.H. (2000). Vps52p, Vps53p, and Vps54p form a novel multisubunit complex required for protein sorting at the yeast late Golgi. Mol. Biol. Cell *11*, 305–323.

Cosson, P., and Letourneur, F. (1997). Coatomer (COPI)-coated. vesicles: role in intracellular transport and protein sorting. Curr. Opin. Cell Biol. *9*, 484–487.

Costanzo, M.C., *et al.* (2000). The Yeast Proteome Database (YPD) and *Caenorhabditis elegans* Proteome Databases (WormPD): comprehensive resources for the organization and comparison of model organism protein information. Nucleic Acids Res. *28*, 73–76.

Cowles, C.R., Emr, S.D., and Horazdovsky, B.F. (1994). Mutations in the *VPS45* gene, a *SEC1* homolog, result in vacuolar protein sorting defects and accumulation of membrane vesicles. J. Cell Sci. *107*, 3449–3459.

Cowles, C.R., Snyder, W.B., Burd, C.G., and Emr, S.D. (1997). Novel Golgi to vacuole delivery pathway in yeast: identification of a sorting determinant and required transport component. EMBO J. *16*, 2769–2782.

Cunningham, K.W., and Fink, G.R. (1994). Calcineurin-dependent growth control in *Saccharomyces cerevisiae* mutants lacking *PMC1*, a homolog of plasma membrane Ca^{2+} ATPases. J. Cell Biol. *124*, 351–363.

Cunningham, K.W., and Fink, G.R. (1996). Calcineurin inhibits *VCX1*-dependent H^+/Ca^{2+} exchange and induces Ca^{2+} ATPases in *Saccharomyces cerevisiae*. Mol. Cell. Biol. *16*, 2226–2237.

Cyert, M.S., Kunisawa, R., Kaim, D., and Thorner, J. (1991). Yeast has homologs (*CNA1* and *CNA2* gene products) of mammalian calcineurin, a calmodulin-regulated phosphoprotein phosphatase. J. Cell Biol. *124*, 351–363.

Cyert, M.S., and Thorner, J. (1992). Regulatory subunit (*CNB1* gene product) of yeast CA^{2+}/calmodulin-dependent phosphoprotein phosphatases is required for adaptation to pheromone. Mol. Cell. Biol. *12*, 3460–3469.

Dean, N. (1995). Yeast glycosylation mutants are sensitive to aminoglycosides. Proc. Natl. Acad. Sci. USA *92*, 1287–1291.

Dulic, V., and Reizman, H. (1990). *Saccharomyces cerevisiae* mutants lacking a functional vacuole are defective for aspects of the pheromone response. J. Cell Sci. *97*, 517–525.

Farcasanu, I.C., Hirata, D., Tsuchiya, E., Nishiyama, F., and Miyakawa, T. (1995). Protein phosphatase 2B of *Saccharomyces cerevisiae* is required for tolerance to manganese in blocking the entry of ions into the cell. Eur. J. Biochem. *232*, 712–717.

Fisher von Mollard, G., Nothwehr, S.F., and Stevens, T.H. (1997). The yeast v-SNARE Vti1p mediates two vesicle transport pathways through interactions with the t-SNARE Sed5p and Pep12p. J. Cell Biol. *137*, 1511–1542.

Garrett-Engele, P., Moilanan, B., and Cyert, M.S. (1995). Calcineurin, the Ca^{2+}/calmodulin-dependent protein phosphatase, is essential in yeast mutants with cell integrity defects and in mutants that lack a functional vacuolar H^+-ATPase. Mol. Cell. Biol. *15*, 4103–4114.

Gomes de Mesquita, D.S., Bart van den Hazel, H., Bouwman, J., and Woldringh, C.L. (1996). Characterization of new vacuolar segregation mutants, isolated by screening for loss of proteinase B self-activation. Eur. J. Cell Biol. *71*, 237–247.

Grote, E., and Novick, P.J. (1999). Promiscuity in Rab-SNARE interactions. Mol. Biol. Cell *10*, 4149–4161.

Hemenway, C.S., Dolinski, K., Cardenas, M.E., Hiller, H.A., Jones, E.W., and Heitman, J. (1995). *vph6* mutants of *Saccharomyces cerevisiae* require calcineurin for growth and are defective in vacuolar H^+-ATPase assembly. Genetics *141*, 833–844.

Holthuis, J.C.M., Nichols, B.J., Dhruvakumar, S., and Pelham, H.R.B. (1998). Two syntaxin homologues in the TGN/endosomal system of yeast. EMBO J. *17*, 113–126.

Horazdovsky, B.F., Busch, G.R., and Emr, S.D. (1994). *VPS21* encodes a rab5-like GTP binding protein that is required for the sorting of yeast vacuolar proteins. EMBO J. *13*, 1297–1309.

Horazdovsky, B.F., Davies, B.A., Seaman, M.J., McLaughlin, S.A., Yoon, S., and Emr, S.D. (1997). A sorting nexin-1 homologue, Vps5p, forms a complex with Vps17p and is required for recycling the vacuolar protein-sorting receptor. Mol. Biol. Cell *8*, 1529–1541.

Horazdovsky, B.F., DeWald, D.B., and Emr, S.D. (1995). Protein transport to the yeast vacuole. Curr. Opin. Cell Biol. *7*, 544–551.

Hu, T., Kao, C., Hudson, R.T., Chen, A., and Draper, R.K. (1999). Inhibition of secretion by 1,3-cyclohexanebis(methylamine), a dibasic compound that interferes with coatomer function. Mol. Biol. Cell *10*, 921–933.

Hudson, R.T., and Draper, R.K. (1997). Interaction of coatomer with aminoglycoside antibiotics: evidence that coatomer has at least two dilysine binding sites. Mol. Biol. Cell *8*, 1901–1910.

Jones, E.W. (1977). Proteinase mutants of *Saccharomyces cerevisiae*. Genetics *85*, 23–33.

Klionski, D.J. (1998). Nonclassical protein sorting to the yeast vacuole. J. Biol. Chem. *273*, 10807–10810.

Klionski, D.J., Herman, P.K., and Emr, S.D. (1990). The fungal vacuole: composition, function, and biogenesis. Microbiol. Rev. *54*, 266–292.

Lang, T., Schaeffeler, E., Bernreuther, D., Bredschneider, M., Wolf, D.H., and Thumm, M. (1998). Aut2p and Aut7p, two novel microtubule-associated proteins, are essential for delivery of autophagic vesicles to the vacuole. EMBO J. *17*, 3597–3607.

Lewis, M.J., Nichols, B.J., Prescianotto-Baschong, C., Riezman, H., and Pelham, H.R.B. (2000). Specific retrieval of the exocyst SNARE Snc1p from early yeast endosomes. Mol. Biol. Cell *11*, 23–38.

Liu, Y., *et al.* (1991). The *Saccharomyces cerevisiae* genes (*CMP1* and *CMP2*) encoding calmodulin-binding proteins homologous to the catalytic subunit of mammalian protein phosphatase 2B. Mol. Gen. Genet. *227*, 52–59.

Lupas, A., Van Dyke, M., and Stock, J. (1991). Predicting coiled coils from protein sequences. Science *252*, 1162–1164.

Marcusson, E.G., Horazdovsky, B.F., Cereghino, J.L., Gharakhanian, E., and Emr, S.D. (1994). The sorting receptor for yeast vacuolar carboxypeptidase Y is encoded by the *VPS10* gene. Cell *77*, 579–586.

Marks, B., and McMahon, H.T. (1998). Calcium triggers calcineurin-dependent synaptic vesicle recycling in mammalian nerve terminals. Curr. Biol. *8*, 740–749.

Marschall, L.G., Jeng, R.L., Mulholland, J., and Stearns, T. (1996). Analysis of Tub4p, a yeast γ-tubulin-like protein: implications for microtubule-organizing center function. J. Cell Biol. *134*, 443–454.

Matheos, D., Kinsbury, T., Ahsan, U., and Cunningham, K. (1997). TCN1p/Crz1p, a calcineurin-dependent transcription factor that differentially regulates gene expression in *Saccharomyces cerevisiae*. Genes Dev. *11*, 3445–3458.

Mendoza, I., Rubio, F., Rodriguez-Navarro, A., and Pardo, J.M. (1994). The protein phosphatase calcineurin is essential for NaCl tolerance of *Saccharomyces cerevisiae*. J. Biol. Chem. *269*, 8792–8796.

Mulholland, J., Konopka, J., Singer-Kruger, B., Zerial, M., and Botstein, D. (1999). Visualization of receptor-mediated endocytosis in yeast. Mol. Biol. Cell *10*, 799–817.

Nakamura, T., Liu, Y., Hirata, D., Namba, H., Harada, S., Hirokawa, T., and Miyakawa, T. (1993). Protein phosphatase type 2B (calcineurin)-mediated, FK506-sensitive regulation of intracellular ions in yeast is an important determinant for adaptation to high salt stress conditions. EMBO J. *12*, 4063–4071.

Nichols, B.J., Ungermann, C., Pelham, H.R.B., Wickner, W.T., and Haas, A. (1987). Homotypic vacuolar fusion mediated by t- and v-SNAREs. Nature *387*, 199–202.

Pelham, H.R.B. (1999). SNAREs and the secretory pathway: lessons from yeast. Exp. Cell Res. *247*, 1–8.

Piper, R.C., Bryant, N.J., and Stevens, T.H. (1997). The membrane protein alkaline phosphatase is delivered to the vacuole by a route that is distinct from the *VPS*-dependent pathway. J. Cell Biol. *138*, 531–545.

Piper, R.C., Cooper, A.A., Yang, H., and Stevens, T.H. (1995). *VPS27* controls vacuolar and endocytic traffic through a prevacuolar compartment in *Saccharomyces cerevisiae*. J. Cell Biol. *131*, 603–617.

Piper, R.C., Whitters, E.A., and Stevens, T.H. (1994). Yeast Vps45p is a Sec1p-like protein required for the consumption of vacuole-targeted, post-Golgi transport vesicles. Eur. J. Cell Biol. *65*, 305–318.

Pozos, T.C., Sekler, I., and Cyert, M.S. (1996). The product of *HUM1*, a novel yeast gene, is required for vacuolar Ca^{2+}/H^{+} exchange and is related to mammalian Na^{+}/Ca^{2+} exchangers. Mol. Cell. Biol. *16*, 3730–3741.

Rambourg, A., Gachet, E., Clermont, Y., and Kepes, F. (1996). Modifications of the Golgi apparatus in *Saccharomyces cerevisiae* lacking microtubules. Anat. Rec. *246*, 162–168.

Raymond, C.K., Howald-Stevenson, I., Vater, C.A., and Stevens, T.H. (1992). Morphological classification of the yeast vacuolar protein sorting mutants: evidence for a prevacuolar compartment in class E *vps* mutants. Mol. Biol. Cell *3*, 1389–1402.

Redding, K., Holcomb, C., and Fuller, R.S. (1991). Immunolocalization of Kex2 protease identifies a putative late Golgi compartment in the yeast *Saccharomyces cerevisiae*. J. Cell Biol. *113*, 527–538.

Rieder, S.E., and Emr, S.D. (1997). A novel RING finger protein complex essential for a late step in protein transport to the yeast vacuole. Mol. Biol. Cell *8*, 2307–2327.

Roberts, C.J., Raymond, C.K., Yamashiro, C.T., and Stevens, T.H. (1991) Methods for studying the yeast vacuole. In: Guide to Yeast Genetics and Molecular Biology, ed. C. Guthrie and G.R. Fink, San Diego, CA: Academic Press, 644–661.

Robinson, J.S., Klionsky, D.J., Banta, L.M., and Emr, S.D. (1988). Protein sorting in *Saccharomyces cerevisiae*: isolation of mutants defective in the delivery and processing of multiple vacuolar hydrolases. Mol. Cell. Biol. *8*, 4936–4948.

Rothman, J.H., Howald, I., and Stevens, T.H. (1989). Characterization of genes required for protein sorting and vacuolar function in the yeast *Saccharomyces cerevisiae*. EMBO J. *8*, 2057–2065.

Rothman, J.H., and Stevens, T.H. (1986). Protein sorting in yeast: mutants defective in vacuole biogenesis mislocalize vacuolar proteins into the late secretory pathway. Cell *47*, 1041–1051.

Seaman, M.N.J., McCaffery, J.M., and Emr, S.D. (1998). A membrane coat complex essential for endosome-to-Golgi retrograde transport in yeast. J. Cell Biol. *142*, 665–681.

Sherman, F. (1991) Getting started with yeast. In: Guide to Yeast Genetics and Molecular Biology, ed. C. Guthrie and G.R. Fink, San Diego, CA: Academic Press, 3–22

Sikorski, R.S., and Hieter, P. (1989). A system of shuttle vectors and yeast host strains designed for efficient manipulation of DNA in *Saccharomyces cerevisiae*. Genetics *122*, 19–27.

Singer-Kruger, B., Stenmark, H., Düsterhöft, A., Philippsen, P., Yoo, J.-S., Gallwitz, D., and Zerial, M. (1994). Role of three Rab5-like GTPases, Ypt51p, Ypt52p, and Ypt53p, in the endocytic and vacuolar protein sorting pathways. J. Cell Biol. *125*, 283–298.

Smith, A.M., Archer, J.E., and Solomon, F. (1998). Regulation of tubulin polypeptides and microtubule function: Rki1p interacts with the β-tubulin binding protein Rbl2p. Chromosoma *107*, 471–478.

Stathopoulos, A.M., and Cyert, M.S. (1997). Calcineurin acts through the *CRZ1/TCN1*-encoded transcription factor to regulate gene expression in yeast. Genes Dev. *11*, 3432–3444.

Stepp, J.D., Huang, K., and Lemmon, S.K. (1997). The yeast adaptor protein complex, AP-3, is essential for the efficient delivery of alkaline phosphatase by the alternate pathway to the vacuole. J. Cell Biol. *139*, 1761–1774.

Tanida, I., Hasegawa, A., Iida, H., Ohya, Y., and Anraku, Y. (1995). Cooperation of calcineurin and vacuolar H^{+}-ATPase in intracellular Ca^{2+} homeostasis of yeast cells. J. Biol. Chem. *270*, 10113–10119.

TerBush, D.R., Maurice, T., Roth, D., and Novick, P. (1996). The exocyst is a multiprotein complex required for exocytosis in *Saccharomyces cerevisiae*. EMBO J. *15*, 6483–6494.

TerBush, D.R., and Novick, P. (1995). Sec6, Sec8, and Sec15 are components of a multisubunit complex which localizes to small bud tips in *Saccharomyces cerevisiae*. J. Cell Biol. *130*, 299–312.

Van Den Hazel, H.B., Kielland-Brandt, M.C., and Winther, J.R. (1996). Review: biosynthesis and function of yeast vacuolar proteases. Yeast *12*, 1–16.

Vida, T.A., and Emr, S.D. (1995). A new vital stain for visualizing vacuolar membrane dynamics and endocytosis in yeast. J. Cell Biol. *128*, 779–792.

Voos, W., and Stevens, T.H. (1998). Retrieval of resident late-Golgi membrane proteins from the prevacuolar compartment of *Saccharomyces cerevisiae* is dependent on the function of Grd19p. J. Cell Biol. *140*, 577–590.

Wada, Y., Ohsumi, Y., and Anraku, Y. (1992). Genes for directing vacuolar morphogenesis in *Saccharomyces cerevisiae*. J. Biol. Chem. *267*, 18665–18670.

Waters, M.G., and Pfeffer, S.R. (1999). Membrane tethering in intracellular transport. Curr. Opin. Cell Biol. *11*, 453–459.

Wendland, B., Emr, S.D., and Riezman, H. (1998). Protein traffic in the yeast endocytic and vacuolar protein sorting pathways. Curr. Opin. Cell Biol. *10*, 513–522.

Wiesman, L.S., Emr, S.D., and Wickner, W.T. (1990). Mutants of *Saccharomyces cerevisiae* that block intervacuole vesicular traffic and vacuole division and segregation. Proc. Natl. Acad. Sci. USA *97*, 1076–1080.

Wilsbach, K., and Payne, G.S. (1993). Dynamic retention of TGN proteins in *Saccharomyces cerevisiae*. Trends Cell Biol. *3*, 462–431.

Withee, J.L., Mulholland, J., Jeng, R., and Cyert, M.S. (1997). An essential role of the yeast pheromone-induced Ca^{2+} signal is to activate calcineurin. Mol. Biol. Cell *8*, 263–277.

Withee, J.L., Sen, R., and Cyert, M.S. (1998). Ion tolerance of *Saccharomyces cerevisiae* lacking the Ca^{2+}/CaM-dependent phosphatase (calcineurin) is improved by mutations in *URE2* or *PMA1*. Genetics *149*, 865–878.